NASA Technical Memorandum 4581

Vestibular Afferent Responses to Linear Accelerations in the Alert Squirrel Monkey

Christopher J. Somps, *Ames Research Center, Moffett Field, California*
Robert H. Schor, *University of Pittsburgh, Pittsburgh, Pennsylvania*
David L. Tomko, *Ames Research Center, Moffett Field, California*

AUGUST 1994

National Aeronautics and
Space Administration

Ames Research Center
Moffett Field, California 94035-1000

Vestibular Afferent Responses to Linear Accelerations in the Alert Squirrel Monkey

CHRISTOPHER J. SOMPS, ROBERT H. SCHOR,* AND DAVID L. TOMKO

Ames Research Center

Summary

The spontaneous activity of 40 otolith afferents and 44 canal afferents was recorded in 4 alert, intact squirrel monkeys. Polarization vectors and response properties of otolith afferents were determined during static re-orientations relative to gravity and during Earth-horizontal, sinusoidal, linear oscillations. Canal afferents were tested for sensitivity to linear accelerations. For regular otolith afferents, a significant correlation between upright discharge rate and sensitivity to dynamic acceleration in the horizontal plane was observed. This correlation was not present in irregular units. The sensitivity of otolith afferents to both static tilts and dynamic linear acceleration was much greater in irregularly discharging units than in regularly discharging units. The spontaneous activity and static and dynamic response properties of regularly discharging otolith afferents were similar to those reported in barbiturate-anesthetized squirrel monkeys. Irregular afferents also had similar dynamic response properties when compared to anesthetized monkeys. However, this sample of irregular afferents in alert animals had higher resting discharge rates and greater sensitivity to static tilts. The majority of otolith polarization vectors were oriented near the horizontal in the plane of the utricular maculae; however, directions of maximum sensitivity were different during dynamic and static testing. Canal afferents were not sensitive to static tilts or linear oscillations of the head.

Introduction

Electrophysiological recordings from eighth-nerve canal and otolith afferents have been made in a variety of species and under a variety of conditions (e.g., refs. 1–4). Most such experiments have been conducted under barbiturate or other anesthesia, frequently after removal of portions of the cerebrum and cerebellum overlying the nerve. In only a few instances (refs. 5–7) have such recordings been made in intact, alert monkeys, and then only testing the response of horizontal canal afferents to angular head rotations. This study reports recordings from vestibular afferents in intact, unanesthetized squirrel monkeys during whole-body static tilts and dynamic linear acceleration.

The response of both canal and otolith afferents has been most thoroughly studied using the barbiturate-anesthetized squirrel monkey preparation (e.g., refs. 3, 8, 9). Because these studies were conducted in anesthetized animals in which the recording site was surgically exposed, the results may not represent the activity of afferents in alert, intact monkeys. For example, anesthesia may depress the activity of vestibular efferents, which have been shown to modulate the sensitivity and dynamic response properties of primary afferents (ref. 10).

The primary goal of the present study was to measure the response of otolith afferents to dynamic linear oscillations and static tilts in alert squirrel monkeys. Resting, tilt-coding, and dynamic response properties were determined and compared to those reported for a similar population of otolith afferents in barbiturate-anesthetized squirrel monkeys (refs. 1, 8, 9).

In addition, the present experiments allowed us to investigate the response of canal afferents to linear acceleration. Past reports (refs. 3, 4, 11, 12) indicate that canal afferents can show responses to linear accelerations, particularly those produced by whole-body tilt. However, Goldberg and Fernandez (ref. 3) showed that in their squirrel monkey preparation, canal sensitivity to tilt was probably a temperature-induced artifact arising from the exposure of the recording site. This exposure was believed to produce thermal gradients across the temporal bone of sufficient magnitude to generate convective flows in the canal lumen during head tilt or linear acceleration. In contrast, Perachio and Correia (ref. 4) reported canal afferent responses to small-angle head tilts in unanesthetized, decerebrated gerbils with intact labyrinths, which suggests a physiological rather than artifactual source. In the present study, a closed-chamber system was used to record canal afferents in intact, alert animals; thus, it is believed that a faithful representation of the animal's natural signaling properties has been recorded.

*University of Pittsburgh, Pittsburgh, Pennsylvania

Methods

Animals

Four adult male squirrel monkeys (*S. sciureus*), weighing 0.9–1.0 kg were the subjects of this study. Under surgical anesthesia, a modified Trent Wells recording chamber was aseptically fixed to the skull over a craniotomy (~1 cm diameter) centered right of the midsagittal plane at the stereotaxic coordinates P1.5 mm, L3.0–6.0 mm. The craniotomy was sealed by placing a thin covering of medical-grade silastic over the exposed dura inside the recording chamber. At the same time, a 1/4-inch stainless steel head-fixation bolt was aseptically fixed to the occiput as described previously (ref. 13). This device enabled painless, reproducible head restraint during recording sessions. Animals were allowed to recover for at least two weeks prior to recording. The care and treatment of animals conformed to the guidelines of the Ames Research Center Animal User's Guide (AHB 7180-1) and the National Institutes of Health (NIH) Guide for the Care and Use of Laboratory Animals.

Unit Recordings

In each three-hour recording session, the animal was seated in a primate chair in an upright position with its head fixed. In a few cases, animals were given a subclinical dose (1 mg oral or intramuscular) of Valium to relax them during the recording sessions. Three of the four animals had their heads fixed so that the Horsley–Clarke plane was Earth-horizontal. The remaining animal was fixed with its head tilted 15 deg nose down. A stainless steel guide tube (outside diameter (O.D.) 0.8 mm) was inserted through the silastic seal at the base of the recording chamber, guided through the dura and the tentorium, and then securely attached to the recording chamber. An electrolytically sharpened tungsten micro-electrode (O.D. 0.25 mm, 1.5–3.0 Megohm at 1 KHz, insulated with Epoxylite) or a small-bore glass micro-electrode filled with 2M NaCl (O.D. 0.25 mm, 3.0–6.0 Megohm at 1 KHz, Perachio and Correia, 1983b) was then advanced out of the guide tube, through the cerebellum and into the brainstem lateral to the vestibular nuclei. Units were recorded between P1.0–P2.0 and L5.0–L7.0. In medial tracks, vestibular afferent fibers were isolated 4–5 mm below the ventral surface of the cerebellum, while in more lateral tracks, afferent fibers were encountered 0.5–1.0 mm below the flocculus. Because the animals were to be used in additional tests, histological corroboration of electrode tracks was not done.

Apparatus and Stimulus Characteristics

All experiments were conducted at NASA's Vestibular Research Facility (VRF) at Ames Research Center using a spring-driven, linear sled. The animal coordinate convention used in these studies was centered at the Horsley–Clarke stereotaxic 0 and has been described previously (ref. 13); the +Z axis was directed upward through the top of the head, the +X axis forward through the nose, and the +Y axis out the left ear. The monkey, seated in the primate chair, was held in a specimen test container (STC) that was mounted to the sled carriage by a three-axis gimbal (fig. 1). The innermost, or internal, positioning axis was fixed relative to the test container and was aligned with the animal's Z axis. Rotations about this axis (η) produced yaw rotations of the animal within the STC. The middle, Earth-horizontal, positioning axis allowed the animal to be rotated in a vertical plane determined by the orientation of the internal axis. Thus, when the internal axis was rotated so the monkey's line of sight was along the horizontal axis (η = 90 deg or 270 deg), rotations about the horizontal axis (φ) produced roll. When the internal axis was rotated so the horizontal axis passed through the animal's ears (η = 0 deg or 180 deg), rotations about the horizontal axis produced pitch. The outermost, or vertical, positioning axis was fixed to the sled, and rotations about this axis (θ) allowed the horizontal axis to be positioned relative to the direction of linear motion.

Isolated units were tested for sensitivity to angular accelerations in the three canal planes, static linear accelerations produced by tilts relative to gravity, and dynamic linear accelerations produced by oscillations along an Earth-horizontal axis. Angular accelerations were generated by rotating animals manually in the following orientations: upright, with rotations about the vertical axis ($\eta = \varphi = 0$) producing angular accelerations approximately in the plane of the horizontal canals; upright, with the animal yawed η = 45 deg using the internal axis and rotated about the horizontal axis (producing angular motion in the plane of the right anterior and left posterior canal); and upright, with the animal yawed η = –45 deg using the internal axis and rotated about the horizontal axis (producing angular motion in the plane of the right posterior and left anterior canal). Cells that responded vigorously to angular head motion in any of these three planes were presumed to be canal afferents.

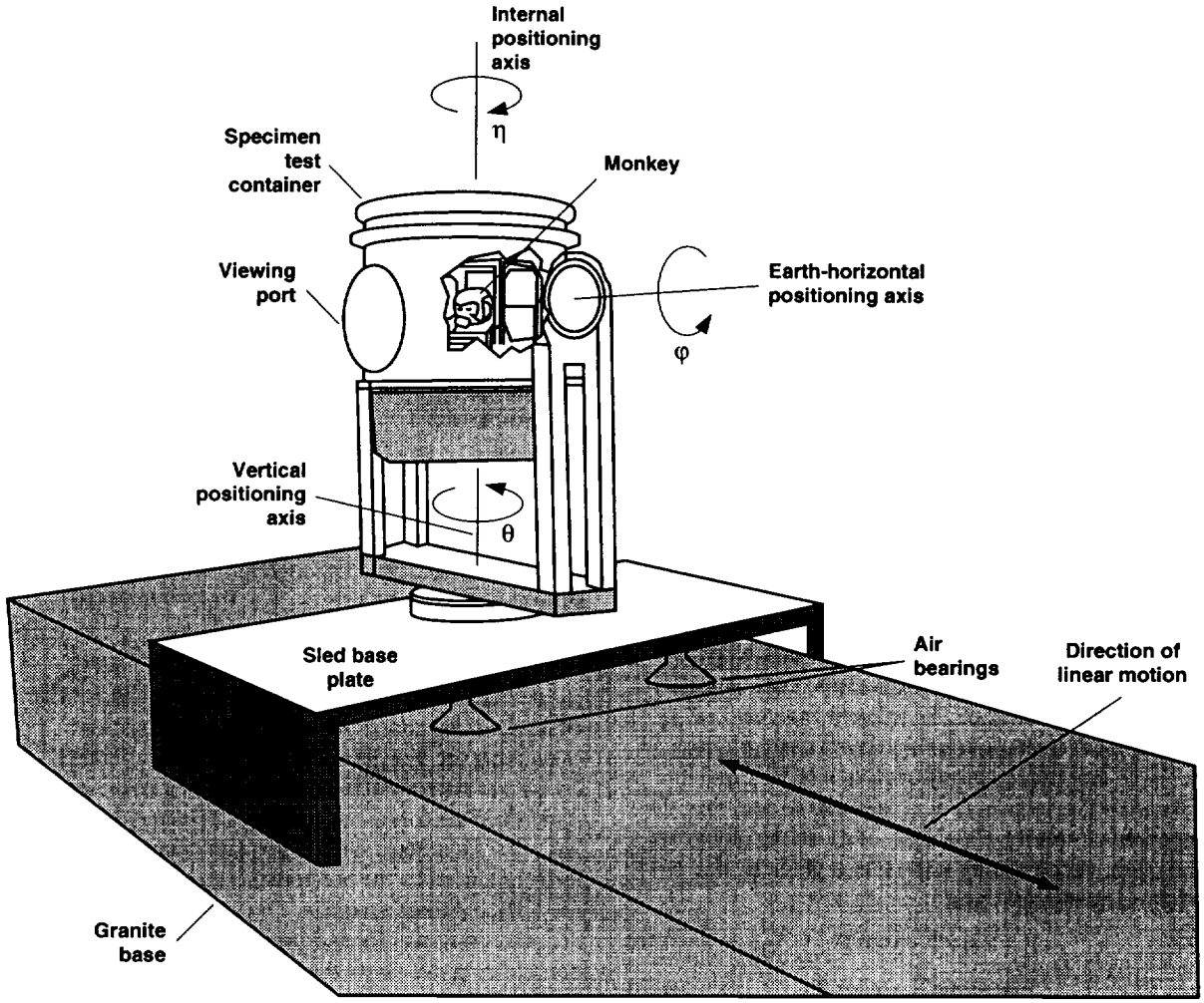

Figure 1. NASA's VRF spring-driven, linear sled. The 3-axis gimbal allows rotations (η) about an internal axis, rotations (φ) about an Earth-horizontal axis, and rotations (θ) about a vertical axis. For the orientation of the animal and STC shown, η = φ = θ = 0. η is 0 when the animal faces the viewing port; φ is 0 when the animal and STC are upright; and θ is 0 when the Earth-horizontal axis is aligned with the axis of motion as shown. The direction of linear acceleration was along the length of the sled.

In the second test, animals were statically positioned relative to gravity. An internal axis position of $\eta = 0$ deg or $\eta = 90$ deg was chosen. The animal was then held at $\varphi = 0$ deg, 90 deg, and –90 deg. In this way static discharge rates were recorded with the monkey in five static orientations relative to gravity: upright, nose down, nose up, right ear down, and left ear down. The majority of static tilts were 90 deg; however, less stable units were only subjected to 20-deg tilts.

Finally, animals were sinusoidally oscillated along an Earth-horizontal axis. The vertical axis was used to position the animal relative to the direction of linear motion. Upright animals were stimulated along the interaural (Y) axis ($\theta = 0$ deg), and along the naso-occipital (X) axis ($\theta = 90$ deg). Animals were then pitched nose down and stimulated along the dorsoventral (Z) axis. Three more Z-axis trials were then done (if cell remained isolated)—nose up, left ear down, and right ear down. Each isolated cell, in addition to being tested statically, was tested at one of two frequencies, 0.5 Hz or 1.5 Hz. Peak accelerations were between 0.26 g and 0.36 g (1 g = 980 cm/s^2), and 5–15 cycles were recorded for each animal position. Cells that responded to static tilts or dynamic linear accelerations but not angular motion were presumed to be otolith afferents.

Data Acquisition and Analysis

Unit discharges were amplified (by 10^4) and discriminated. Interspike intervals (10 μs resolution) and sled acceleration (sampled at 200 Hz) were recorded and stored for later analysis.

For each cell, spontaneous discharge frequency and regularity were determined with the animal upright and stationary. Given that T is the measured interspike interval, the instantaneous discharge frequency, d, was defined as

$$d = 1/T \tag{1}$$

and discharge regularity was assessed by calculating the coefficient of variation, CV,

$$CV = S/\overline{T} \tag{2}$$

where S is the standard deviation and $\overline{T}$ is the average of n ($25 < n < 150$) interspike intervals.

Responses to static head tilts– Static tilt data were only collected from the three animals whose heads were held in the Earth-horizontal stereotaxic plane. Data analysis was similar to previous otolith afferent analyses (ref. 1). If the direction of maximum sensitivity to static tilt is given by a single unit polarization vector $\mathbf{f_s} = (x,y,z)$, and the acceleration due to gravity is normalized to one, then the component of gravity, F (in units of g), acting along this polarization vector during static tilts is given by one of the following relationships:

$$F = x\sin P - z\cos P \tag{3a}$$

$$F = -y\sin R - z\cos R \tag{3b}$$

where P is the angle of pitch from upright and R is the angle of roll from upright.

Assuming that the discharge rate, d, is a linear function of F, then for any head position relative to gravity

$$d = s_S F + d_O \tag{4}$$

where s_S is the afferent's static sensitivity (in impulses/sec/g) and d_O is the 0-force discharge rate (i.e., the discharge rate when the cell's polarization vector is orthogonal to gravity).

The static sensitivities along the X, Y, and Z axes are derived from equations (3) and (4) and are expressed as

$$s_S x = (d_P - d_{-P})/2\sin P \tag{5a}$$

$$s_S y = -(d_R - d_{-R})/2\sin R \tag{5b}$$

$$s_S z = \left[(d_P + d_{-P})/2 - d_{up}\right]/(1-\cos P) \tag{5c}$$

$$s_S z = \left[(d_R + d_{-R})/2 - d_{up}\right]/(1-\cos R) \tag{5d}$$

where d_P and d_{-P} are the discharge rates measured for pitches of P degrees nose down and nose up, respectively, and d_R and d_{-R} are the discharge rates measured for rolls of R degrees right ear down and left ear down, respectively. d_{up} is the discharge rate when the animal is upright. When responses to both roll and pitch tilts were obtained, the vertical response, $s_S z$, was determined by averaging the two values obtained from equations (5c) and (5d). The components of the polarization vector, $\mathbf{f_s} = (x,y,z)$, and the static sensitivity, s_S, were determined from the definition of the polarization vector as a unit vector of length 1.

$$s_S = \sqrt{\left((s_S x)^2 + (s_S y)^2 + (s_S z)^2\right)} \tag{6a}$$

$$\mathbf{f_s} = (x,y,z) = (s_S x, s_S y, s_S z)/s_S \tag{6b}$$

Responses to dynamic linear motion– The dynamic sensitivity, polarization vector orientation, and response phase were obtained by analyzing the responses of afferents to sinusoidal oscillations (0.5 Hz and 1.5 Hz) along an Earth-horizontal axis. The equations for calculating the dynamic sensitivity and polarization vector can be derived in a manner similar to the case of static tilt. Two forces are present: a constant downward force due to gravity, and the perpendicular sinusoidal force produced by the horizontal sinusoidal motion. The gravitational force produces a mean afferent discharge rate; the sinusoidal force produces a sinusoidal modulation of firing rate about this mean, and the modulation amplitude is governed by the component of the linear acceleration in the direction of the polarization vector (analogous to equations (3) and (4) for the static case).

When the animal's X axis is aligned so the animal faces the direction of motion and the animal is statically pitched about the interaural axis, the amplitude of the sinusoidal acceleration along the dynamic polarization vector, $\mathbf{f_d} = (x,y,z)$, is given by

$$F = a(x\cos P + z\sin P) \tag{7a}$$

where a is the amplitude of the horizontal linear acceleration (units of g). When the animal is aligned so the left ear faces the direction of motion and the animal is positioned in roll, the amplitude of the sinusoidal acceleration along $\mathbf{f_d} = (x,y,z)$ is

$$F = a(y\cos R - z\sin R) \tag{7b}$$

These sinusoidal oscillations produced a sinusoidal modulation of the firing rate of sensitive afferents. The amplitude and phase of this response were determined by

fitting a sine wave to a binned representation of the instantaneous firing rates. In some cases, irregular afferents were silent during a portion of the motion cycle. In these instances, the response was sinusoidally extrapolated below the baseline and then fit with a sine function.

Analogous to equation (4), the amplitude of the sinusoidal response, $\hat{d}$, is simply the dynamic sensitivity, s_d (in impulses/sec/g), times the amplitude of the applied acceleration as given by equations (7a) or (7b). For simplicity, we determined the X component of s_d with the animal upright (R = P = 0) and facing the direction of motion; the Y component was similarly determined in the upright animal, but using equation (7b) and the animal oriented so the left ear faced the motion. To obtain the Z component, the responses to oppositely directed rolls and pitches were subtracted. Thus it follows that

$$s_d x = \hat{d}_{P=0}/a \tag{8a}$$

$$s_d y = \hat{d}_{R=0}/a \tag{8b}$$

$$s_d z = \left(\hat{d}_P - \hat{d}_{-P}\right)/2a \sin P \tag{8c}$$

$$s_d z = \left(\hat{d}_{-R} - \hat{d}_R\right)/2a \sin R \tag{8d}$$

In those cases where $s_d z$ was determined using both pitch and roll tilts, the two values were averaged. Once $s_d x$, $s_d y$, and $s_d z$ were determined, s_d and the dynamic response vector orientation $\mathbf{f_d} = (x,y,z)$ could be determined using equations (6a) and (6b) (replacing s_s with s_d). From responses to oscillations along the X and Y axes alone, we computed the projection of the three-dimensional polarization vector onto the horizontal plane, and determined a horizontal sensitivity s_h. Also, some units were not tested along the Z axis.

The one animal whose head was fixed 15-deg nose down was treated mathematically as though it was identical to the other three animals. Thus, when the animal was upright, ($\varphi = 0$) P = 15 deg, and when the animal was pitched about the interaural axis P = φ + 15 deg. In three units from this animal, $s_d z$ was not determined because the cells were not held through roll or pitch tilts. In these cases, $s_d x$ was estimated by assuming the term $a s_d z \times \sin 15$ deg was 0 in the equation

$$s_d x = \left(\hat{d} - a s_d z \sin 15\,\text{deg}\right)/a \cos 15\,\text{deg} \tag{9}$$

As we will show below, the phase of the sinusoidal response for most units was essentially independent of the orientation of the stimulus axis. Accordingly, we computed the phase of the response by averaging the phases obtained for each stimulus direction.

Statistical tests– Unless indicated otherwise, a two-tailed Student's t-test was employed at the 95% confidence level for statistical comparisons between means. Linear correlations between parameters were tested for statistical significance at the 95% confidence level using the Pearson product-moment correlation coefficient.

Results

General

All 84 cells described here were recorded from a small, circumscribed area (~1 mm anteroposterior × ~1 mm dorsoventral) between L5 and L7. Spontaneous discharge rates in stationary animals were stable and showed no variation during saccades or other eye movements; they appeared to carry no eye position signal. Responses to rotations and linear accelerations were polarized. If rotation (or acceleration) in one direction increased neural firing, a stimulus in the opposite direction decreased it (fig. 2).

Neural responses could be divided into two classes. One showed a response to static tilt or linear accelerations, but not to angular accelerations in the horizontal plane; the other showed no dependence on static position or horizontal linear oscillation, but responded vigorously to angular head rotations in the plane of one of the three semicircular canals. We presume that responses in the first class arise from otolith afferents, while responses in the second class come from semicircular canal afferents.

All units reported here were spontaneously active, firing in the absence of a deliberate stimulus. Discharge waveforms were positive and were generally triphasic (positive–negative–positive). Responses varied between 75–200 μvolts in amplitude and 0.5–0.7 msec in width. Of the 84 putative vestibular afferents recorded, 40 were classified as otolith afferents and 44 were classified as canal afferents. Additional afferents in each class were observed, but not recorded.

Isolating otolith afferents was more difficult than isolating canal afferents. About half of the otolith afferents encountered were isolated long enough to record their activity; and fewer than this could be stabilized during roll and pitch tilts. Canal afferents were encountered more frequently and were isolated more easily, response amplitudes were generally larger, and stability was better than for otolith afferents. Additional canal afferents were not recorded because, during the fairly short 3-hour recording sessions, the focus was to isolate and record otolith afferents.

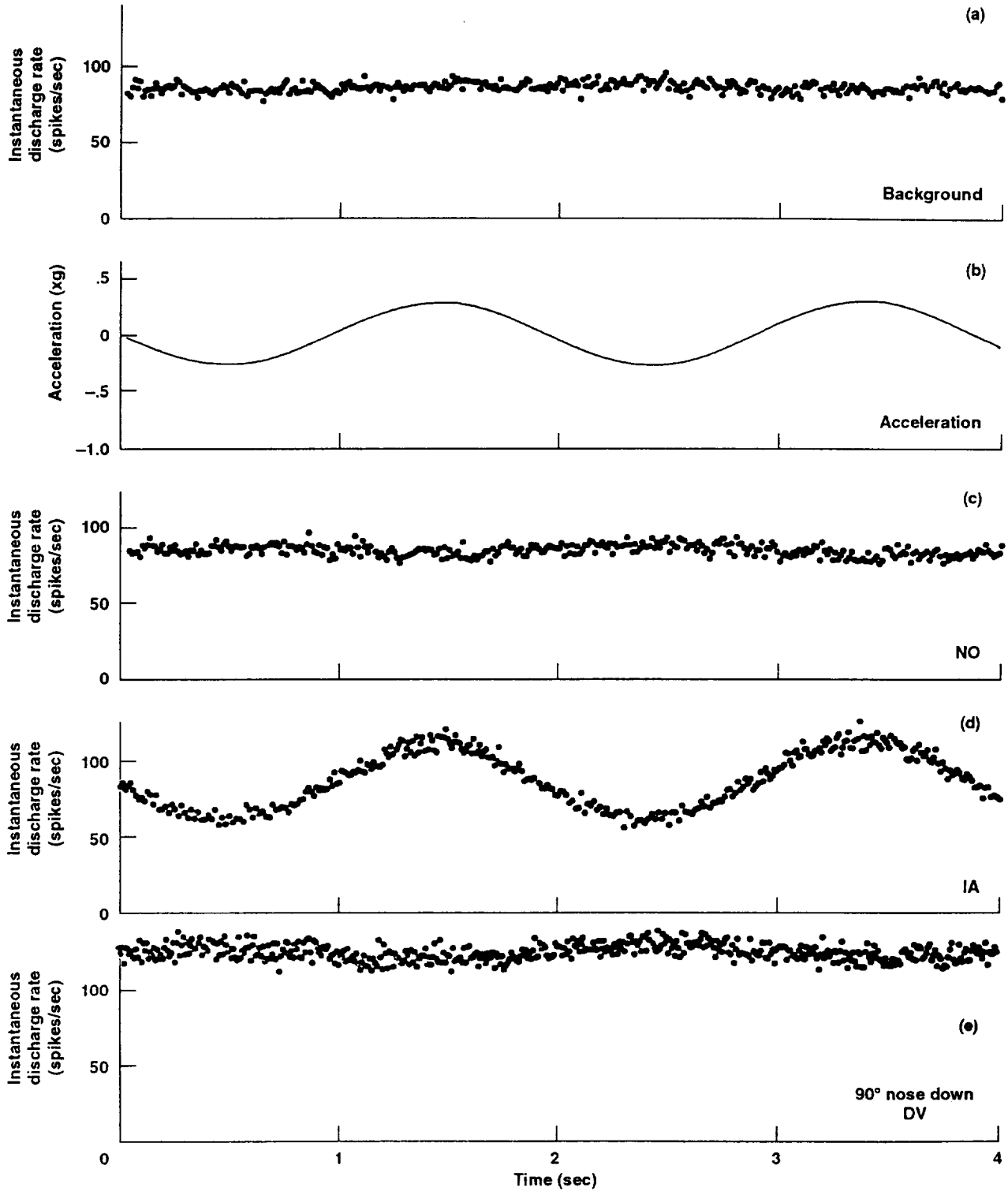

Figure 2. Instantaneous discharge rates of an otolith afferent subjected to Earth-horizontal, sinusoidal, linear oscillations; (a) when the animal is upright and stationary, (b) the stimulus acceleration, (c) when the animal is upright and facing the direction of linear motion (θ = 90 deg, naso-occipital stimulus), (d) when the animal is perpendicular to the direction of linear motion (θ = 0 deg, interaural stimulus), and (e) when the animal is tilted 90 deg nose down (φ = 90 deg) and the direction of linear motion is along the long axis of the animal (θ = 90 deg, dorsoventral stimulus).

Otolith Afferents

Static responses– Activity was recorded in 40 otolith units; 36 from the three animals whose heads were aligned with the stereotaxic plane and 4 from the animal whose head was positioned 15 deg nose down. Twenty-five (63%) had very regular discharge rates (CV < 0.1) while animals were stationary and in an upright position (fig. 3(a)). The remainder had CVs between 0.1 and 0.8. The average upright discharge rate of the regular afferents was 67 spikes/sec and was not significantly different from that of the irregular afferents, which was 88 spikes/sec ($p > 0.05$) (fig. 3(b)).

Eight otolith afferents remained isolated during the whole-body tilts required to fully characterize response sensitivity and orientation in three dimensions. Four of these were irregularly discharging units and four were regularly discharging units. For regular afferents, the average response sensitivity to static tilts was 39 spikes/sec/g. Irregular afferents had clearly greater sensitivities, 133 spikes/sec/g, when compared to regular afferents.

Unit polarization vectors were also determined for these eight isolated afferents. Only one vector was directed downward, and vectors were evenly split between ipsilateral and contralateral orientations. Five afferents were directed toward the back of the head and three were directed toward the front of the head. Half of the vectors lay within 30 deg of the horizontal plane and six out of eight lay within 40 deg of the horizontal plane.

Dynamic responses in the horizontal plane– Of the forty isolated afferents, 39 were tested dynamically at either 0.5 Hz or 1.5 Hz, and response sensitivity and phase were based on the modulated component of the response (see Methods). The response sensitivity to linear oscillations in the horizontal (XY) plane, s_h, was calculated for 34 afferents (19 regular and 15 irregular). In the remaining five afferents, sensitivities were determined for stimulation along either the X or Y axis, but not both. Of the regular afferents, 10 were tested at 0.5 Hz, 9 were tested at 1.5 Hz, and the average sensitivities in the horizontal plane were 47 and 58 spikes/sec/g, respectively. For the regularly discharging afferents (pooled across 0.5 and 1.5 Hz tests) there was a significant ($p < 0.01$) positive product-moment correlation between the upright, resting discharge rate and s_h (slope = 0.55, $r = 0.58$) (fig. 4(a)). Of the irregular afferents, 1 was tested at 0.5 Hz and 14 were tested at 1.5 Hz. The unit tested at 0.5 Hz had a horizontal plane sensitivity of 171 spikes/sec/g, and the cells tested at 1.5 Hz had an average horizontal plane sensitivity of 221 spikes/sec/g. In contrast to the regular units, there was not a significant correlation ($p > 0.05$) between resting discharge rate and s_h for irregular afferents (fig 4(b)).

For stimuli in the horizontal plane, response phase appeared relatively constant regardless of the orientation of the animal relative to the direction of motion (fig. 5). Response phases for stimuli along the X and Y directions, ϕ_x and ϕ_y, were measured in 18 (of 19) regular afferents and 15 irregular afferents. Neither regular nor irregular afferents showed a significant ($p > 0.05$) correlation between ϕ_x or ϕ_y and the angle between the direction of the stimulus and the direction of maximum sensitivity in the horizontal plane. This would be expected if the afferent were encoding acceleration along a single fixed direction; response amplitude would vary with the cosine of the angle between the stimulus direction and vector orientation, while response phase should be constant (to within 180 deg where the stimulus changes from excitatory to inhibitory). Response phase was therefore defined as an average of the component phases ϕ_x, ϕ_y, and ϕ_z (see Methods).

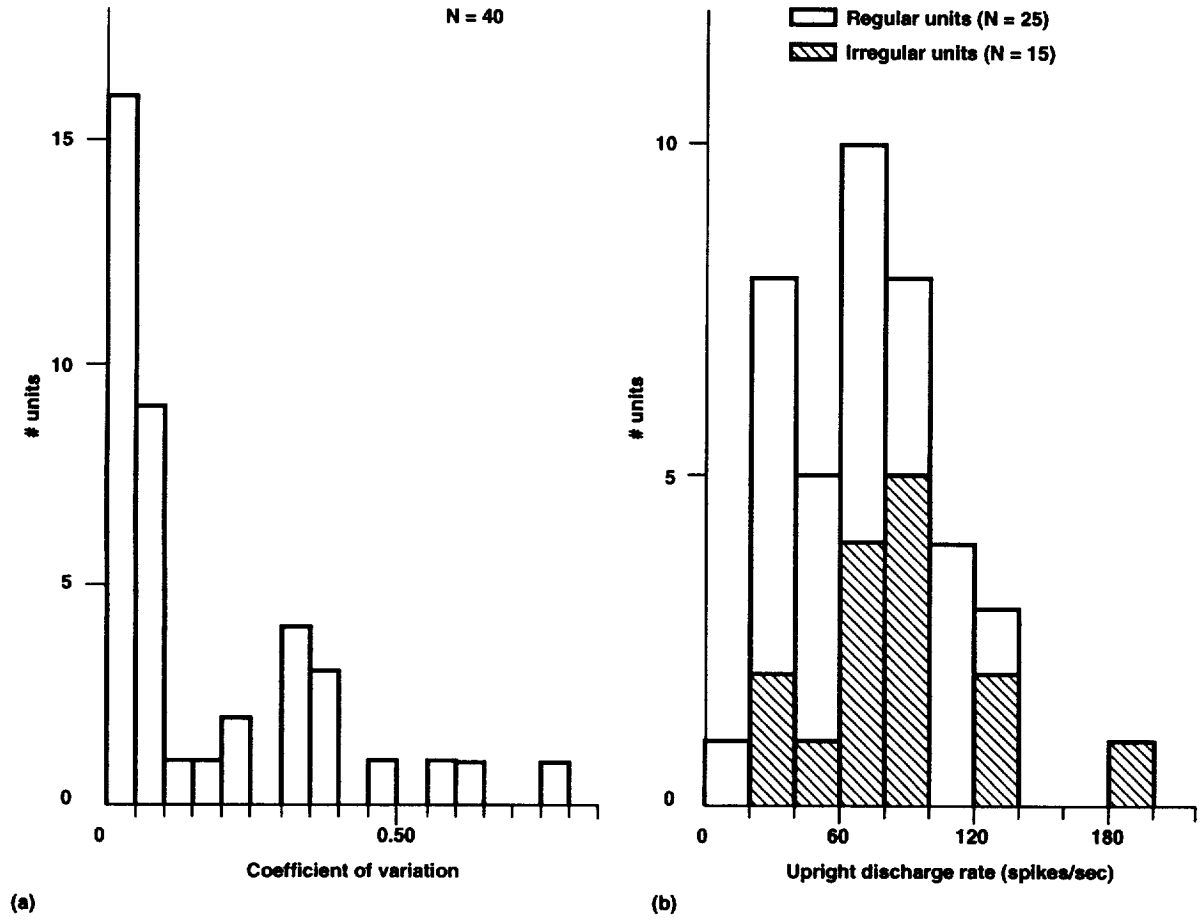

Figure 3. (a) Distribution of CVs (bin width = 0.05) for 40 otolith afferents. (b) Cumulative histogram (bin width = 20 spikes/sec) showing the upright discharge rate for 25 regular afferents and 15 irregular afferents.

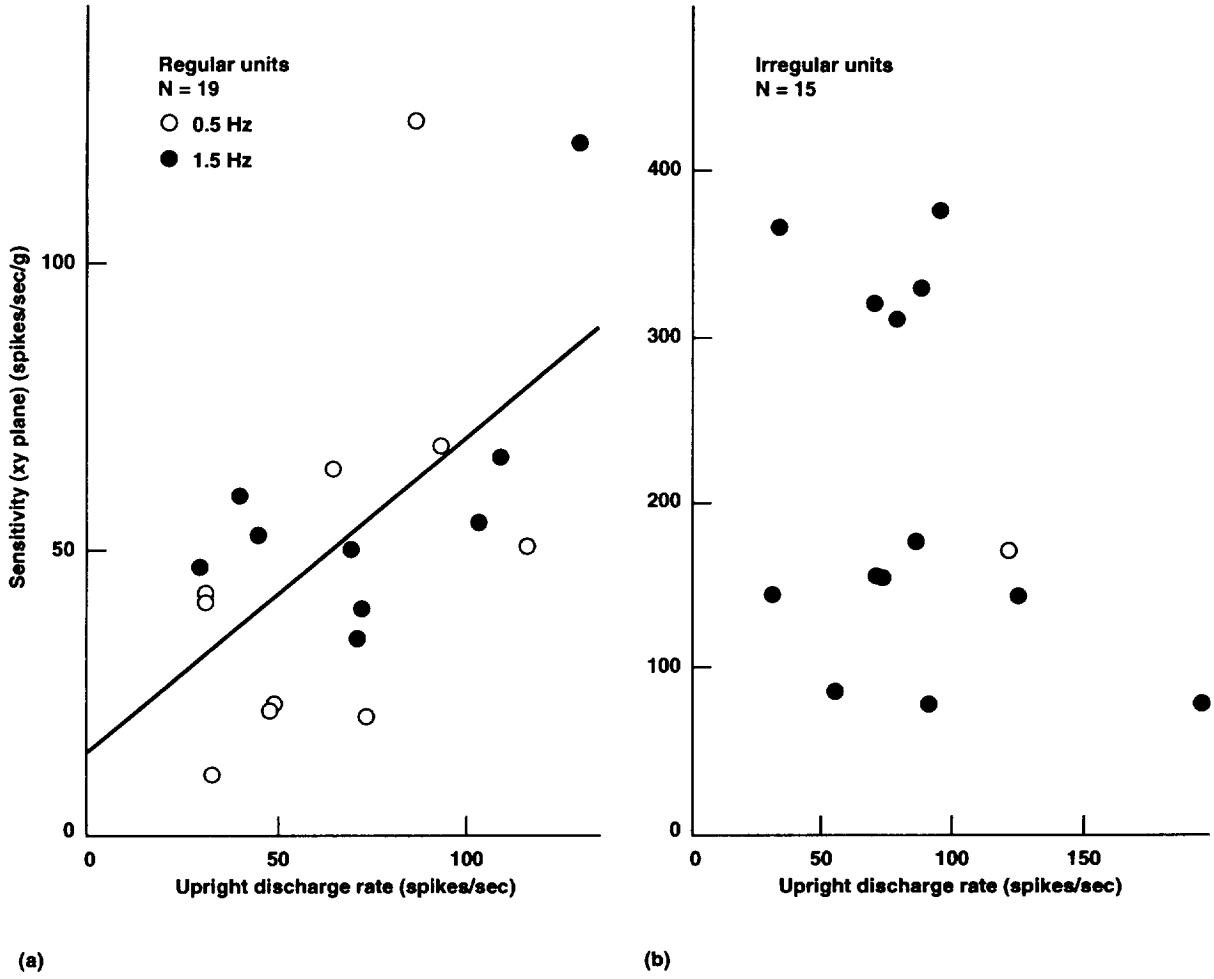

Figure 4. Scatter diagrams showing the relation between upright spontaneous discharge rate and s_h for (a) regular afferents ($r = 0.58$, slope = 0.55 g^{-1}), and (b) irregular afferents. In both cases, horizontal plane sensitivities are pooled from both 0.5 (open circles) and 1.5 Hz (closed circles) stimulus tests.

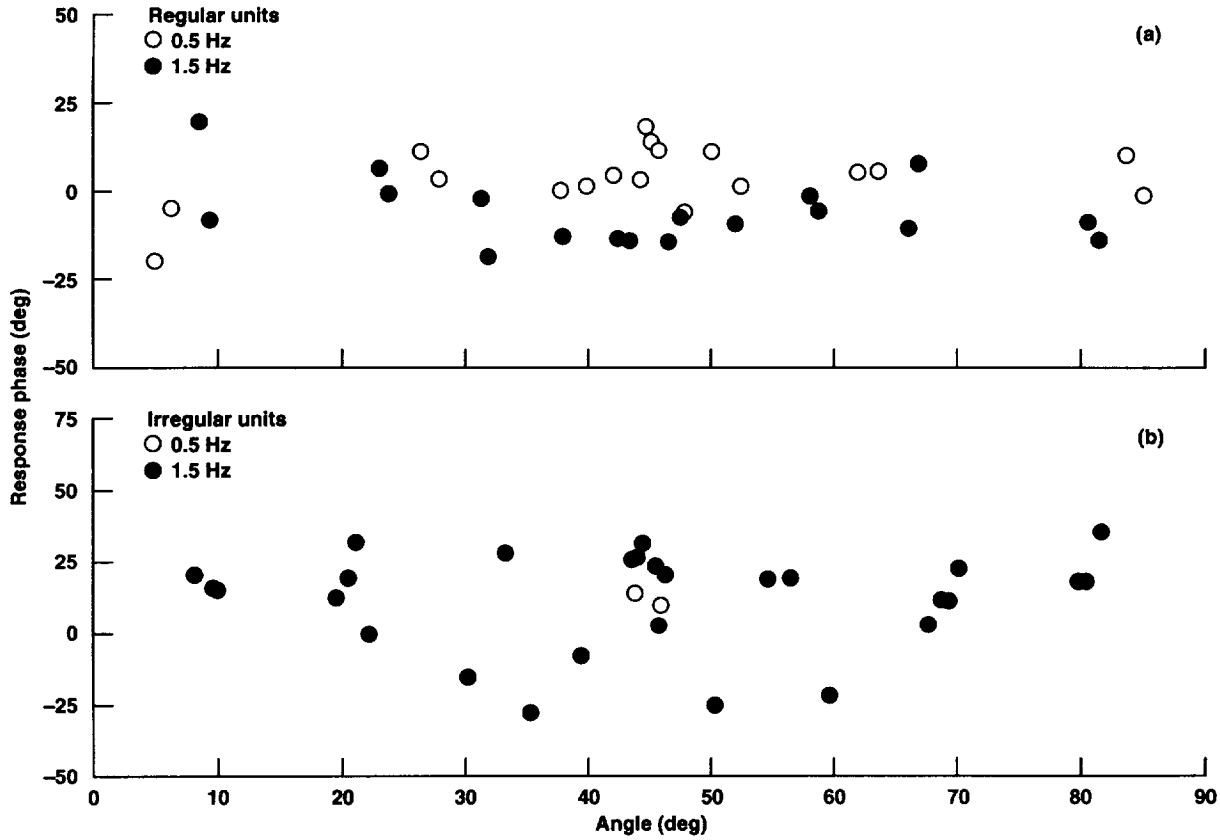

Figure 5. Scatter diagrams showing relationship between response phases ϕ_X and ϕ_Y and the angle between the direction of maximum sensitivity in the horizontal plane and the direction of motion for (a) regular, and (b) irregular afferents. Phases are corrected for 180-deg phase differences. Open circles indicate 0.5 Hz responses, and closed circles indicate 1.5 Hz responses.

Of the 19 regular afferents tested, ϕ_X and ϕ_Y were determined in 18: 9 at 0.5 Hz and 9 at 1.5 Hz. At 0.5 Hz, the average phase for responses in the horizontal plane was 4.1 deg, and at 1.5 Hz the average phase was –5.7 deg (positive values indicate phase leads). Of the 15 irregular afferents, 1 was tested at 0.5 Hz and 14 were tested at 1.5 Hz. For the unit stimulated at 0.5 Hz the phase of the response was 12.8 deg, and for the cells tested at 1.5 Hz the average phase was 12.6 deg.

Dynamic responses in three dimensions–

Sensitivity and phase: The three-dimensional (3-D) sensitivity was calculated for 19 otolith afferents: 10 regular and 9 irregular. Response phase, which was the average of the component phases (n = 1, 2, or 3), was determined in 39: 24 regular and 15 irregular. For regular afferents, average response sensitivity to linear oscillations of 0.5 and 1.5 Hz was 54 (n = 5) and 61 (n = 5) spikes/sec/g, respectively; values slightly increased relative to static tilt values (fig. 6(a)). Response phase decreased with increasing stimulus frequency between 0.5 (n = 11) and 1.5 Hz (n = 13) (fig. 6(b)).

For irregular afferents, the average response sensitivity to linear oscillations of 0.5 and 1.5 Hz was 173 (n = 1) and 266 (n = 8) spikes/sec/g, respectively; again, values slightly increased relative to those observed with static tilts (fig. 6(a)). Irregular afferents had significantly greater ($p < 0.01$ at 1.5 Hz) sensitivities (3–4 times greater) and phase leads (10–15 deg) when compared to regular afferents.

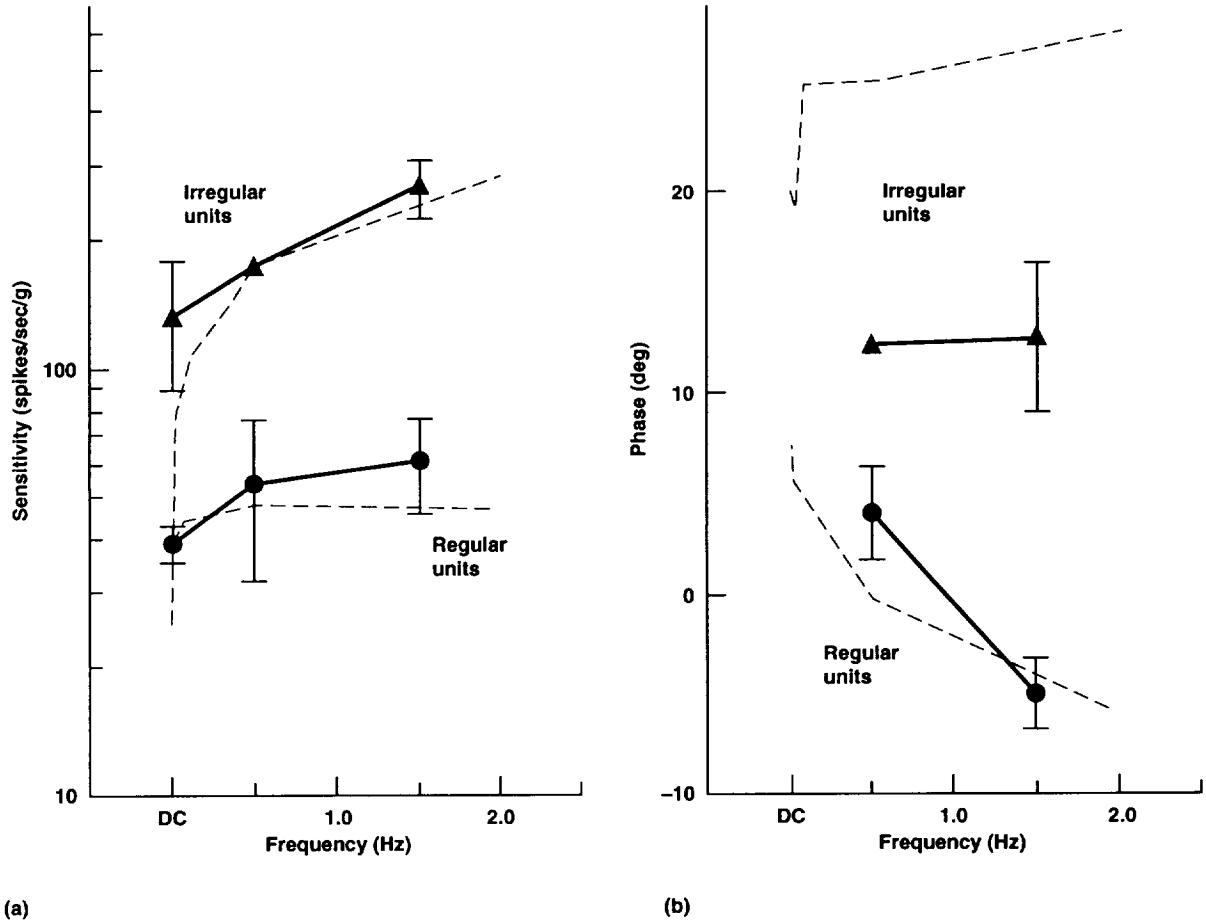

Figure 6. Three-dimensional (a) sensitivity and (b) phase of regular (circle) and irregular (triangle) afferents as a function of stimulus frequency. Sensitivity points are the average of regular (DC, n = 4; 0.5 Hz, n = 5; 1.5 Hz, n = 5) and irregular (DC, n = 4; 0.5 Hz, n = 1; 1.5 Hz, n = 8) afferents. Phase points are the average of regular units (0.5 Hz, n = 11; 1.5 Hz, n = 13) and the average of irregular units (0.5 Hz, n = 1; 1.5 Hz, n = 14). Error bars are ±1 SEM. Positive phase values depict phase leads. For comparison, thin dashed lines in the background show sensitivities and phases for regular and irregular afferents in anesthetized squirrel monkeys (ref, 9; excitatory stimulation). In six (of eight) units, 3-D sensitivities to static tilts were measured using 90-deg tilts. In the remaining two units, z component sensitivity was calculated using both pitch and roll tilts of 20 deg (see equations in Methods).

Direction of maximum sensitivity: Unit polarization vectors, $\mathbf{f_d}$, were calculated for 19 afferents from component sensitivities measured during dynamic stimulation at 0.5 and 1.5 Hz. These unit polarization vectors were projected onto the 3 orthogonal planes as shown in figures 7(a)–7(c) (polarization vectors from static tests are also shown) to provide views from the back, top, and right side of the head, respectively.

Sixteen (84%) afferents were directed above the horizontal, 13 (68%) were directed ipsilaterally, and 12 (63%) were directed forward. The polarization vectors of 14 afferents lie within 30 deg of the horizontal plane when stimulated dynamically (fig. 7(a)). The average angle of these vectors relative to the horizontal plane was 5.6 deg, describing a plane tilted in a ventromedial-dorsolateral orientation. Five afferents had dynamic polarization vectors oriented at angles greater than 30 deg above the horizontal plane; of these, 3 had polarization vectors directed toward the ipsilateral side of the head. Nine (of 19) polarization vectors lie within 30 deg of the frontal plane, while only 3 vectors were oriented within 30 deg of the sagittal plane when stimulated dynamically (fig. 7(b)).

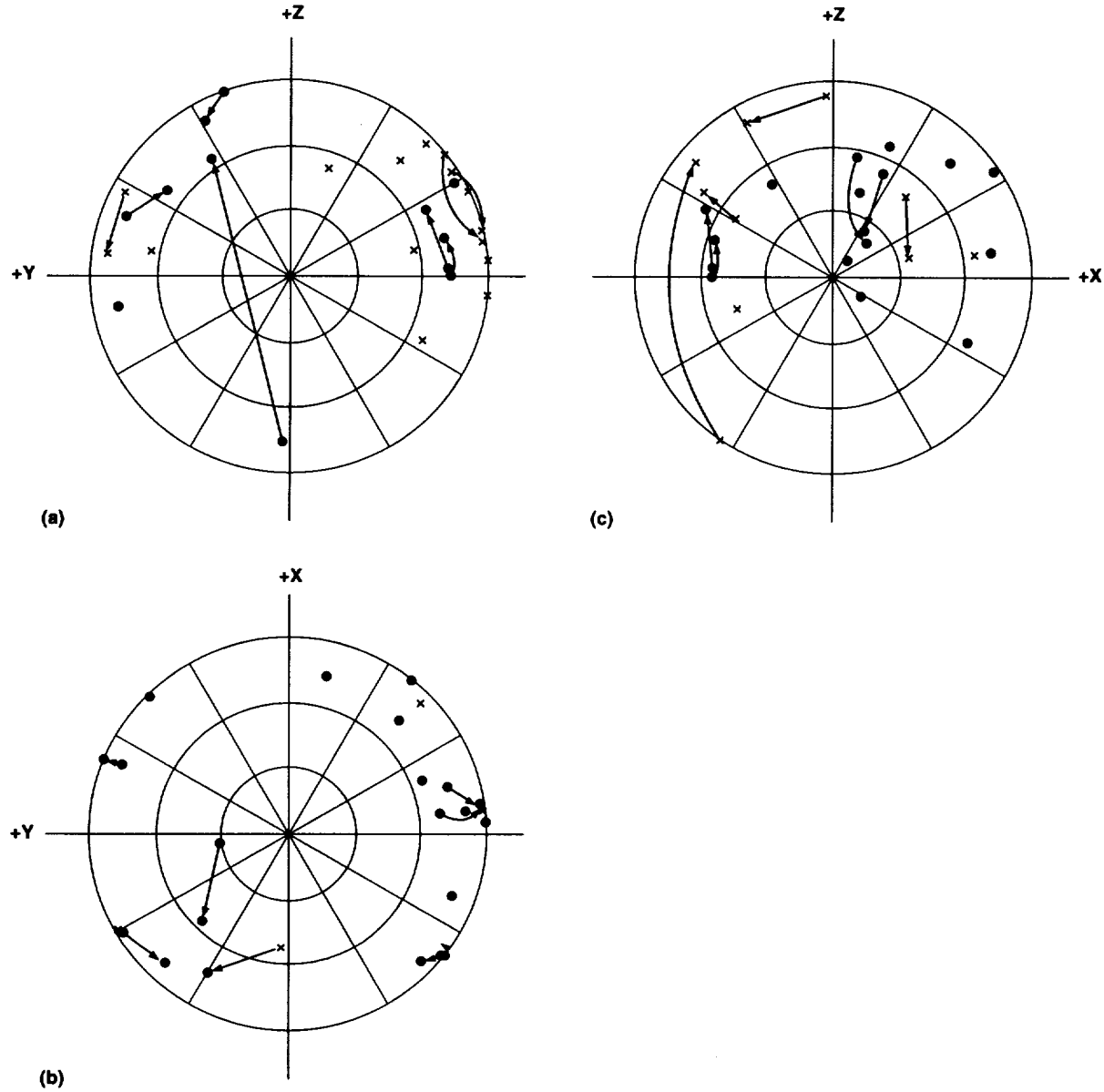

Figure 7. Unit polarization vectors for 19 afferents were projected onto the YZ, YX, and XZ planes, providing views from the (a) back of the head, (b) top of the head, and (c) right side of the head. X's indicate polarization vectors with components directed into the page, and dots indicate vectors with components directed out of the page. Radii are shown every 30 deg, and concentric circles are shown at 1/3, 2/3, and 1. For eight afferents, polarization vectors were calculated from sensitivities to static tilts and Earth-horizontal, sinusoidal, linear head motion. Lines connect polarization vectors $\mathbf{f}_s$ *and* $\mathbf{f}_d$ *from the same afferent. Arrows point to polarization vectors determined with dynamic stimuli.*

Direction of maximum sensitivity—static versus dynamic– For 8 of the 19 afferents, unit polarization vectors were also calculated from response sensitivities to static tilts, $\mathbf{f_s}$. Six of these units belonged to the population with vectors that lay within 30 deg of the horizontal plane when stimulated dynamically. These 6 afferents showed different directions of maximum sensitivity with static tilts than with dynamic stimulation. The differences were largely confined to the vertical planes (figs. 7(a)–7(c)), averaged 20 deg in the frontal plane and 20 deg in the sagittal plane, and resulted primarily from changes in the z component of the unit polarization vectors. Changes in the orientation of these afferents in the horizontal plane were much smaller, averaging only 5 deg (fig. 7(b)). With static tilts, the remaining two afferents showed differences in the direction of $\mathbf{f_s}$ when compared to $\mathbf{f_d}$ in all three orthogonal planes; differences in the frontal, horizontal, and sagittal planes averaged 76, 32, and 61 deg, respectively. There was no clear difference in the amount of change observed for regular and irregular afferents. However, the unit with the largest reorientation was an irregular afferent. This cell showed a 144 deg change in the frontal plane.

Canal Afferents

Forty-four afferents sensitive to angular accelerations were recorded. Each was tested for sensitivity to rotation in the horizontal and vertical canal planes (see Methods). Fifteen afferents were sensitive only to vertical rotations that excite the animal's ipsilateral posterior canal (posterior canal afferents (PCA)). Fourteen were sensitive only to vertical rotations that excite the ipsilateral anterior canal (anterior canal afferents (ACA)). Fifteen afferents were sensitive only to yaw rotation (horizontal canal afferents (HCA)). There were 31 regularly discharging and 13 irregularly discharging fibers. Of these 44 afferents, 38 (11 PCA, 13 ACA, and 14 HCA) were tested for sensitivity to sinusoidal, translational motion in the horizontal plane (±0.26–0.36 g), and 4 were tested for sensitivity to static tilts relative to gravity. No canal afferent exhibited any measurable changes in discharge rate in response to dynamic or static linear accelerations.

Discussion

General Response Properties

The vestibular afferent fibers of this study were all recorded from a small, circumscribed area lateral to the vestibular nuclei where stereotaxic maps show a dense concentration of vestibular afferents. As expected of fibers, units were difficult to isolate and to hold, especially otolith units. Response waveforms were between 75 and 200 μvolts and were triphasic, as reported previously for vestibular afferents (ref. 7). All responses were polarized; firing rates increased for acceleration in one direction and decreased for acceleration in the opposite direction. Canal units responded to rotations in a single canal plane and not to linear head motion or static head tilt. Otolith units responded to linear head motion or head tilt, but not to angular motion. Finally, spontaneous discharge rates in stationary animals were stable despite frequent eye movements. All of the above indicate that our recordings were from primary afferents, and not vestibular nuclei neurons.

Previous studies have shown that cells in the vestibular nuclei can increase firing rates for accelerations in opposing directions (e.g., ref. 15), can fire during both angular and linear accelerations (e.g., ref. 16), and often carry an eye movement signal (e.g., ref. 17). None of these characteristics were observed in our cell population.

The reason for the difference in recording stability between canal and otolith afferents is not clear. Morphological studies (ref. 18) have shown that human canal afferents are, on average, slightly larger than otolith afferents. If also true in the squirrel monkey, this size difference may make otolith-derived fibers somewhat harder to isolate and stabilize than canal afferents. Also, the relative number of otolith and canal fibers may differ in our recording site.

Otolith Response Properties in Alert Animals

Response properties of otolith afferents in the alert squirrel monkey were, on the whole, very similar to those reported previously for anesthetized squirrel monkeys (refs. 1, 8, 9). Both populations showed similar spontaneous discharge characteristics, sensitivity and phase to dynamic stimuli, and, in the case of regular afferents, nearly identical sensitivity to static tilts. However, a striking difference between the two populations was observed in the sensitivity of irregular afferents to static tilts. Irregular afferents in alert animals were roughly six times more sensitive to static tilts than irregular afferents reported by Fernandez and Goldberg (ref. 9) in anesthetized monkeys.

There were slightly more irregular units in our population of otolith afferents—38% compared to ~17% (ref. 1) in anesthetized monkeys. However, the coefficient of variation distributions were otherwise quite similar. Also, the distribution of instantaneous firing rates for otolith afferents in alert, upright squirrel monkeys was similar to the distribution of 0-force discharge rates found in anesthetized animals. Most polarization vectors in the

present study lie near the horizontal plane, implying that the upright and 0-force discharge rates are the same. The only difference was in the average spontaneous discharge rate of irregular afferents, which was 1.5 to 2 times greater in alert compared to anesthetized animals (refs. 1 and 8).

Fernandez et al. (ref. 1) showed a positive correlation between sensitivity to static tilts and 0-force discharge rates in regular units from anesthetized animals. This correlation permits units with higher discharge rates to show larger bidirectional responses. The correlation was absent for irregular afferents. Because of the small number of afferents for which static sensitivities were determined in the present study, a comparison with 0-force discharge was not made. However, the sensitivity of regular afferents to dynamic stimuli in the horizontal plane was positively correlated with upright discharge rate; a similar correlation was absent for irregular afferents. As with the statically tested afferents, most polarization vectors recorded during dynamic testing lay near the horizontal plane, where s_h is roughly equal to s_d and upright discharge rates are equal to 0-force discharge rates. Thus, relationships between discharge rates and sensitivities found in anesthetized animals were also found in alert animals.

The 3-D response sensitivity and phase of regularly discharging afferents across a 0 to 1.5 Hz bandwidth were remarkably similar in alert and anesthetized animals, suggesting that anesthesia has little effect on the dynamic response properties of regularly discharging otolith afferents. The response sensitivity of irregular afferents to 0.5 Hz and 1.5 Hz stimuli were also similar in the two conditions, although response phase leads were smaller in alert animals. In contrast, the mean static response of irregularly discharging units was ~6 times greater than the 23 spikes/sec/g observed in anesthetized animals (ref. 9). This, in conjunction with higher spontaneous discharge rates in alert animals, suggests the possibility that irregular afferents differ from regular ones in their greater sensitivity to anesthesia, as well as their larger fiber size (ref. 19), enhanced response dynamics (ref. 9), and lower excitation thresholds (ref. 20).

Differences in irregular afferent responses in alert and anesthetized animals may reflect different influences of the efferent vestibular system in the two cases. Neuroanatomical studies in the squirrel monkey revealed an efferent vestibular system with neurons located within the brain stem and fibers projecting to the peripheral vestibular labyrinth (ref. 10). Electrical stimulation of these neurons modifies the resting activity and response dynamics in primary afferents, especially in irregular afferents where responses to efferent stimulation are 10–20 times larger than those of regular afferents. The work of Goldberg and Fernandez (ref. 10) suggests that efferent vestibular system neurons modify afferent fiber activity in alert animals. If barbiturate anesthesia significantly modifies efferent neurons, afferent responses to linear accelerations in anesthetized animals might be expected to be different from those in alert animals, especially for irregular afferents, consistent with the findings of the present study. The fact that the effect is most evident during static tilts may reflect a low-pass filtering of efferent influence on otolith primary afferent activity in alert animals. In order to fully understand the irregular afferent sensitivity change in alert animals it will be necessary to characterize a transfer function by measuring dynamic responses at frequencies between 0 and 0.5 Hz.

Polarization Vector Orientation

Approximately 3/4 of the afferents for which unit polarization vectors were calculated from responses to dynamic stimulation had vectors lying within 30 deg of the horizontal (the average tilt angle in a ventromedial-dorsolateral orientation). These polarization vectors correspond to a similar population of afferents whose orientations were reported by Fernandez and Goldberg (ref. 8) to be consistent with an origin on the utricular maculae. Two of the remaining 5 afferents had unit polarization vectors directed in the +Y direction at angles greater than 30 deg above the horizontal. These polarization vectors correspond to a similar population of afferents reported by Fernandez and Goldberg (ref. 8) to be consistent with a saccular origin.

When tested statically, differences in vector orientation were observed. For afferents whose polarization vectors were near the horizontal, changes in direction were largely confined to a plane orthogonal to the horizontal. For polarization vectors oriented >30 deg above the horizontal, changes in orientation were observed in all three orthogonal planes. Although these observations may reflect response nonlinearities and difficulties in the accurate determination of $\mathbf{f_d}$ and $\mathbf{f_s}$, reorientation of polarization vectors with stimulus frequency may also have a physiological basis. Differences in the direction of maximum sensitivity under static and dynamic loads may reflect the inputs from more than one hair cell for each afferent fiber. Neuroanatomical studies have shown that single afferent fibers innervate more than one hair cell (ref. 21) and that these hair cells often have different morphological polarizations (ref. 22). The resultant polarization vector for any afferent fiber is thus a sum of the polarization vectors of each hair cell. With dynamic stimulation, increases in sensitivity relative to static

responses may be different for each innervated hair cell. If the contributing cells have differing polarizations, the afferent fiber's polarization vector will change, as observed in our population of afferents.

Functional Implications

Do either regular or irregular afferents play a preferential role in the production of the linear vestibular ocular reflex (VOR)? The linear VOR (LVOR) is believed to help stabilize visual images on the retina during linear displacements of the head (ref. 13). In upright squirrel monkeys, LVOR sensitivities to sinusoidal, translational motion of 0.5 Hz and 1.5 Hz along the interaural axis were approximately 13 and 15 deg/sec/g, respectively, and peak eye velocity was nearly in phase with peak sled velocity. The results reported here revealed regular afferent response sensitivities in the horizontal plane of 47 and 58 spikes/sec/g at stimulus frequencies of 0.5 and 1.5 Hz, respectively, and afferent responses were roughly in phase with stimulus acceleration. Thus, for regular afferents, peak afferent discharge led maximum eye velocity by approximately 90 deg. Notably, increases in stimulus frequency from 0.5 Hz to 1.5 Hz resulted in a 15–20% increase in the sensitivity of both regular otolith afferents and horizontal eye movements. In contrast, for irregular afferents, response sensitivity increased by ~30% (170 to 220 spikes/sec/g) for stimulus increases from 0.5 to 1.5 Hz; an increase nearly double that of increases in eye movement sensitivity. This suggests that regular afferents preferentially contribute to the LVOR. Recent studies (ref. 23) using more direct methods also suggest that regular afferents provide the majority of inputs to the angular VOR.

Sensitivity of Canal Afferents to Linear Acceleration

Canal afferents have been reported to be sensitive to tilt (refs. 3, 4, 11, 12). In the squirrel monkey (ref. 3) and the cat (ref. 12), this observation was made in anesthetized animals in which the eighth nerve was surgically exposed. Experimental results obtained by Goldberg and Fernandez (ref. 3) suggested that canal afferent sensitivity to head tilt was due to thermal gradients across the semicircular canals produced by the surgical exposure of the vestibular nerve and petrous pyramid. These thermal gradients could theoretically induce density-driven convective flows in the endolymph with changes in linear accelerations, and they were of the correct sign and magnitude to account for the observed sensitivities of the canal afferents to linear accelerations. Perachio and Correia (ref. 24), however, reported that canal afferents in the unanesthetized, decerebrated gerbil were sensitive to static head tilts. The mechanisms underlying these semicircular canal responses were unclear. One possibility is that even in the intact gerbil, temperature gradients exist across the temporal bone and produce canal responses during static head tilts. In the present study, in which animals were alert and the recording sites were isolated from the external environment, canal afferents were not sensitive to linear head motions or static tilts, supporting arguments that canal afferent sensitivity to linear accelerations, at least in the squirrel monkey, is artifactual.

References

1. Fernandez, C.; Goldberg, J. M.; and Abend, W. K.: Response to Static Tilts of Peripheral Neurons Innervating Otolith Organs of the Squirrel Monkey. J. Neurophys., vol. 35, 1972, pp. 978–997.
2. Loe, R. R,; Tomko, D. L.; and Werner, G.: The Neural Signal of Angular Head Position in Primary Afferent Vestibular Nerve Axons. J. Physiol. (Lond.), vol. 230, 1973, pp. 29–50.
3. Goldberg, J. M.; and Fernandez, C.: Responses of Peripheral Vestibular Neurons to Angular and Linear Accelerations in the Squirrel Monkey. Acta Otolaryngol., vol. 80, 1975, pp. 101–110.
4. Perachio, A.; and Correia, M. J.: Response of Semicircular Canal and Otolith Afferents to Small Angle Static Head Tilts in the Gerbil. Brain Res., vol. 280, 1983, pp. 287–298.
5. Miles, F. A.; and Braitman, D. J.: Long-Term Adaptive Changes in Primate Vestibuloocular Reflex.
   II. Electrophysiological Observations on Semicircular Canal Primary Afferents. J. Neurophys., vol. 43, no. 5, 1980, pp. 1426–1436.
6. Keller, E. L.: Behavior of Horizontal Semicircular Canal Afferents in Alert Monkey during Vestibular and Optokinetic Stimulation. Exp. Brain Res., vol. 24, 1976, pp. 459–471.
7. Louie, A. W.; and Kimm, J.: The Response of 8th Nerve Fibers to Horizontal Sinusoidal Oscillations in the Alert Monkey. Exp. Brain Res., vol. 24, 1976, pp. 447–457.
8. Fernandez, C.; and Goldberg, J. M.: Physiology of Peripheral Neurons Innervating Otolith Organs of the Squirrel Monkey. I. Response to Static Tilts and to Long-Duration Centrifugal Force. J. Neurophys., vol. 39, 1976, pp. 970–984.

9. Fernandez, C.; and Goldberg, J. M.: Physiology of Peripheral Neurons Innervating Otolith Organs of the Squirrel Monkey. III. Response Dynamics. J. Neurophys., vol. 39, 1976, pp. 996–1008.

10. Goldberg, J. M.; and Fernandez, C.: Efferent Vestibular System in the Squirrel Monkey: Anatomical Location and Influence on Afferent Activity. J. Neurophys., vol. 43, 1980, pp. 986–1025.

11. Lowenstein, O.: Physiology of Vestibular Receptors. Progress in Brain Research, vol. 37, Basic Aspects of Central Vestibular Mechanisms, Amsterdam, Elsevier, 1972, pp. 121–127.

12. Estes, M. S.; Blanks, R. H. I.; and Markham, C. H.: Physiologic Characteristics of Vestibular First-Order Canal Neurons in the Cat. I. Response Plane Determination and Resting Discharge Characteristics. J. Neurophys., vol. 38, no. 5, 1975, pp. 1232–1249.

13. Paige, G. D.; and Tomko, D. L.: Eye Movement Responses to Linear Head Motion in the Squirrel Monkey. I. Basic Characteristics. J. Neurophys., vol. 65, 1991, pp. 1170–1182.

14. Schor, R. H.; and Angelaki, D. E.: The Algebra of Neural Response Vectors, In the Annals of the New York Academy of Sciences, Vol. 656, Sensing and Controlling Motion: Vestibular and Sensorimotor Function, New York, New York Academy of Sciences, 1992, pp. 190–204.

15. Xerri, C.; Barthelemy, J.; Harlay, F.; Borel, L.; and Lacour, M.: Neuronal Coding of Linear Motion in the Vestibular Nuclei of the Alert Cat. I. Response Characteristics to Vertical Otolith Stimulation. Exp. Brain Res., vol. 65, 1987, pp. 569–581.

16. Blanks, R. H. I.; Anderson, J. H.; and Precht, W.: Response Characteristics of Semicircular Canal and Otolith Systems in the Cat. II. Responses of Trochlear Motoneurons. Exp. Brain Res., vol. 32, 1978, pp. 509–528.

17. Chubb, M. C.; Fuchs, A. F.; and Scudder, C. A.: Neuron Activity in Monkey Vestibular Nuclei during Vertical Stimulation and Eye Movements. J. Neurophys., vol. 52, no. 4, 1984, pp. 724–742.

18. Bergstrom, B.: Morphology of the Vestibular Nerve: III. Analysis of the Calibers of the Myelinated Vestibular Nerve Fibers in Man at Various Ages. Acta Otolaryng., vol. 76, 1973, pp. 180–187.

19. Goldberg, J. M.; and Fernandez, C.: Conduction Times and Background Discharge of Vestibular Afferents. Brain Res., vol. 122, 1977, pp. 545–550.

20. Goldberg, J. M.; Smith, C. E.; and Fernandez, C.: Relation between Discharge Regularity and Responses to Externally Applied Galvanic Currents in Vestibular Nerve Afferents of the Squirrel Monkey. J. Neurophys., vol. 51, 1984, pp. 1236–1256.

21. Lindeman, H. H.: Studies on the Morphology of the Sensing Regions of the Vestibular Apparatus. Ereb. Anat. Entwickl.-gesch., vol. 42, 1969, pp. 1–113.

22. Ross, M. D.; Cutler, L.; Meyer, G.; Lam, T.; and Vaziri, P.: 3-D Components of a Biological Neural Network Visualized in Computer Generated Imagery. Acta Otolaryngol., vol. 109, 1990, pp. 83–92.

23. Minor, L. B.; and Goldberg, J. M.: Vestibular-Nerve Inputs to the Vestibulo-Ocular Reflex: A Functional-Ablation Study in the Squirrel Monkey. J. Neurosci., vol. 11, 1991, pp. 1636–1648.

24. Perachio, A.; and Correia, M. J.: Design for a Slender Shaft Glass Micropipette. J. Neurosci. Meth.; vol. 9, 1983, pp. 287–293.

REPORT DOCUMENTATION PAGE

Form Approved
OMB No. 0704-0188

1. AGENCY USE ONLY *(Leave blank)*	2. REPORT DATE	3. REPORT TYPE AND DATES COVERED
	August 1994	Technical Memorandum

4. TITLE AND SUBTITLE

Vestibular Afferent Responses to Linear Accelerations in the Alert Squirrel Monkey

5. FUNDING NUMBERS

199-16-12

6. AUTHOR(S)

Christopher J. Somps, Robert H. Schor,* and David L. Tomko

7. PERFORMING ORGANIZATION NAME(S) AND ADDRESS(ES)

Ames Research Center
Moffett Field, CA 94035-1000

8. PERFORMING ORGANIZATION REPORT NUMBER

A-94058

9. SPONSORING/MONITORING AGENCY NAME(S) AND ADDRESS(ES)

National Aeronautics and Space Administration
Washington, DC 20546-0001

10. SPONSORING/MONITORING AGENCY REPORT NUMBER

NASA TM-4581

11. SUPPLEMENTARY NOTES

Point of Contact: Christopher J. Somps, Ames Research Center, MS T20-G, Moffett Field, CA 94035-1000; (415) 604-0193
*University of Pittsburgh, Pittsburgh, Pennsylvania

12a. DISTRIBUTION/AVAILABILITY STATEMENT

Unclassified — Unlimited
Subject Category 51

12b. DISTRIBUTION CODE

13. ABSTRACT ***(Maximum 200 words)***

The spontaneous activity of 40 otolith afferents and 44 canal afferents was recorded in 4 alert, intact squirrel monkeys. Polarization vectors and response properties of otolith afferents were determined during static re-orientations relative to gravity and during Earth-horizontal, sinusoidal, linear oscillations. Canal afferents were tested for sensitivity to linear accelerations. For regular otolith afferents, a significant correlation between upright discharge rate and sensitivity to dynamic acceleration in the horizontal plane was observed. This correlation was not present in irregular units. The sensitivity of otolith afferents to both static tilts and dynamic linear acceleration was much greater in irregularly discharging units than in regularly discharging units. The spontaneous activity and static and dynamic response properties of regularly discharging otolith afferents were similar to those reported in barbiturate-anesthetized squirrel monkeys. Irregular afferents also had similar dynamic response properties when compared to anesthetized monkeys. However, this sample of irregular afferents in alert animals had higher resting discharge rates and greater sensitivity to static tilts. The majority of otolith polarization vectors were oriented near the horizontal in the plane of the utricular maculae; however, directions of maximum sensitivity were different during dynamic and static testing. Canal afferents were not sensitive to static tilts or linear oscillations of the head.

14. SUBJECT TERMS	15. NUMBER OF PAGES
Vestibular afferent, Linear acceleration, Squirrel monkey	20
	16. PRICE CODE: A02

17. SECURITY CLASSIFICATION OF REPORT	18. SECURITY CLASSIFICATION OF THIS PAGE	19. SECURITY CLASSIFICATION OF ABSTRACT	20. LIMITATION OF ABSTRACT
Unclassified	Unclassified		